

## NUMERICAL OPTIMIZATION OF DBD PLASMA ACTUATOR OPERATING PARAMETERS FOR ACTIVE WAVE CANCELLATION USING SINUSOIDAL MODULATION

**Regis de Quadros, Sven Grundmann, Cameron Tropea**

Center of Smart Interfaces,  
TU Darmstadt  
Flughafenstraße, 19, 64347, Griesheim, Germany  
quadros@csi.tu-darmstadt.de, grundmann@csi.tu-darmstadt.de, ctropea@csi.tu-darmstadt.de

**Jane Elsemueller, Stefan Ulbrich**

Mathematik,  
TU Darmstadt  
Schloßgartenstraße 7, 64289, Darmstadt  
elsemueller@mathematik.tu-darmstadt.de, ulbrich@mathematik.tu-darmstadt.de

### ABSTRACT

A numerical investigation of active wave cancellation using a pulsed plasma actuator was carried out for a flat-plate boundary layer with an adverse pressure gradient at low Reynolds number. Pulsing was achieved by sinusoidal modulation of the high-frequency plasma excitation voltage. The closed-loop control was implemented in a CFD code (FASTEST). Using a feed-back control algorithm it was found to be sufficient to control only two of the three operation parameters in order to reduce Tollmien-Schlichting waves significantly. A Nelder-Mead-type method for finding a local minimum of a function of several variables and the trust region method NEWUOA (Powell, 2008) based on quadratic models using minimization without derivatives of functions are used in this work. These two unconstrained optimization algorithms have been used to compare the optimum parameters found by each control algorithm.

### INTRODUCTION

In recent years, much attention has been directed towards actively controlling the laminar-turbulent transition process of a boundary layer. The studies on boundary-layer transition to turbulence remain an important subject because the transition causes a substantial rise in friction drag. Generally, transition in a two-dimensional boundary-layer over a flat-plate is dominated by Tollmien-Schlichting (TS) instabilities. This natural process, which occurs under conditions of very low free-stream turbulence, can be classified into either steady or unsteady disturbances in the free-stream flow, such as noise or vortices (Saric, 2007). The perturbations in the boundary-layer are selectively amplified frequencies while propagating downstream along the flat plate. In the first stage of development, the harmonic instabilities are mainly two-dimensional. In a later stage, the development becomes more and more nonlinear and secondary instabilities lead to an increase in the growth of three-dimensional disturbances. These three-dimensional distortions are followed by the turbulent breakdown.

Due to the high level of disturbances and the extreme difficulty to evaluate the derivatives of objective functions in the simulations, the use of methods for unconstrained optimization becomes indispensable in the optimizations of

the involved parameters for the cancellation of TS-waves using plasma actuators. Algorithms for unconstrained optimization have been used extensively to solve parameter estimation problems for almost 40 years. Despite their age they are still the method of choice for many practitioners in the fields of statistics, engineering and the physical and medical sciences because they are easy to code and very easy to use. The crucial issue is finding a better answer quickly. The asymptotic convergence property is in some cases irrelevant. In fact, a frequent aim in the applications is improvement rather than directly optimization.

Furthermore, the authors present results using optimization tools, where variations of only two parameters are necessary to obtain the cancellation of TS-waves over a flat plate. In this paper, the authors focus on the linear stage of the growth of disturbances, where delaying the laminar-turbulent transition by an active control is more easily achievable. The influence of materials, electrical parameters and geometry of the actuator such as electrode size, thickness, electrode gap and others will not be considered in the present paper.

In this work we consider also the algorithm of Nelder and Mead (1965) because it has become the most popular simplex method in practice for unconstrained optimization. The other optimization method investigated in this paper was developed by Powell (2008).

### THE COMPUTATIONAL DOMAIN

The computational domain and the plasma actuator configuration is corresponding to the original experiments as described in (Grundmann, 2006a). Fig. 1 depicts the test section of 0.45m by 0.45m cross section and a length of 2m. The insert on the ceiling of the test section is designed to create a constant, positive pressure gradient, promoting the transition process. A plasma actuator 400mm downstream of the flat plate's leading edge is operated in pulsed mode to artificially induce TS-waves into the boundary layer at a frequency of 110Hz. The second plasma actuator, denoted as control actuator, is positioned 100mm downstream of the excitor. In this work, the body forces created by the excitor and the control actuator are modulated with a sinusoidal function. Two velocity sensors are positioned at  $x=450$ mm

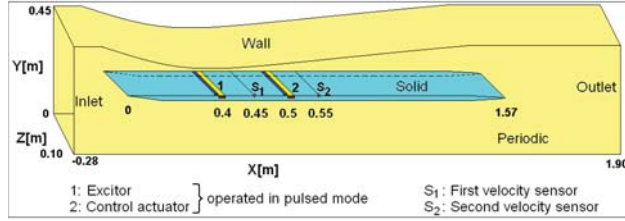


Figure 1: Overview of flow domain, sensor and actuator position and  $x=550\text{mm}$ .

### PLASMA ACTUATOR MODEL

To reduce the computational cost and also to simplify the equations involved in the simulations, this model developed by Jayaraman et al. (2003) and improved and calibrated by Grundmann (2008) assumes that the plasma is present only within a triangular range above the lower electrode and only inside this region can a body force be produced. Assume that no interaction exists between the charge density and the electrical field and that ions which are accelerated by the electrical field pass their entire impulse on to the neutral gas of molecules. Thus, the following expression has been used

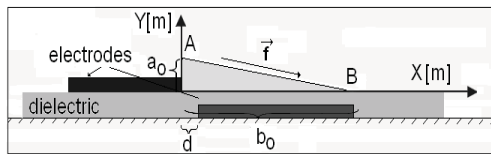


Figure 2: Calibration-based model scheme.

to describe the body force:

$$\vec{f} = \frac{\rho_{c0} V^2}{dV_0} e^{-2(m_1 x + m_2 y)} \vec{n} e_c, \quad (1)$$

where  $m_1$  and  $m_2$  are the gradients of the electric field. The normal vector of the volume strength  $\vec{n}$  depends on the arrangement of the triangular area and it acts constantly over the entire field (see the Fig. (2)). That means that all forces act in the same direction. To model the plasma actuator it is necessary to know the operating voltage  $V$  and the electrode gap  $d$ . The dimensions of the triangular area depends only on the voltage  $V$ . The force is implemented directly in the momentum equations (Navier-Stokes equations) of the solver. The model and also its calibration was presented in (Grundmann, 2006b) and (Quadros et al., 2009).

The sinusoidal modulation used to describe the body-force presented in (1) is given by

$$F^* = bf + \sin[2\pi \frac{v}{\lambda} (t + \phi)] \quad (2)$$

where  $bf$  is the voltage,  $\lambda$  is the wavelength,  $v$  the phase-speed and  $\phi$  the phase-shift. In this work, the frequency and wavelength are constant in the simulations. The body-force and phase-shift are the parameters which need to be optimized. The optimization models used in the current paper are described in the next section.

### OPTIMIZATION MODELS

Two optimization methods will be described and compared to validate the closed-loop control developed in this

work. The Nelder-Mead method is a pattern search algorithm that compares in each iteration the functional values at the vertices and generates a new simplex by replacing the worst vertex by a new one (Nelder, 1965). NEWUOA is a method for unconstrained optimization without derivatives. A local minimum of an objective function  $F(x)$  is calculated by building a quadratic model.

### Closed-loop control

Fig. 3 shows the closed-loop control (CLC) circuit used in the present investigation to attenuate TS-waves. The excitor on the left side excites oscillations in the boundary layer that grow as they travel downstream. 50mm downstream of the excitor a sensor ( $S_1$ ) is positioned. The sensor signal is used to determine the wavelength and amplitude of the TS-waves. If a certain amplitude is exceeded the closed-loop circuit starts to operate. The algorithm follows the steps outline below:

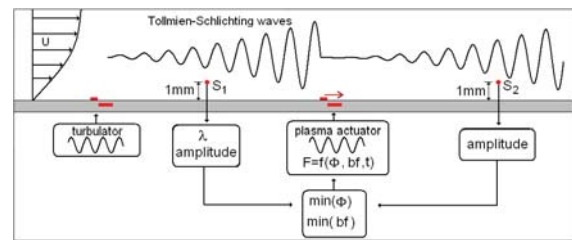


Figure 3: Closed-loop control scheme

1. The signal of the first velocity sensor ( $S_1$ ) indicates when the amplitude of TS-wave ( $\tilde{Y}_i, i = \lambda$ ) is larger than the prescribed amplitude ( $\tilde{Y}_0$ ). Then the initial conditions ( $\Phi_0, bf_0, \Delta_0$ ) are read and the closed-loop circuit starts to operate.
2. These conditions are used in a sinusoidal function  $F^* = f(\Phi, bf, \Delta t)$ , that is coupled to the plasma actuator model, implemented in the Navier-Stokes momentum equation, beginning the process of active wave cancellation.
3. After a period that corresponds to two wavelengths ( $\lambda = \frac{v}{f}$ ), the signal of the second velocity sensor ( $S_2$ ) is used to analyze the amplitude of the attenuated wave. If the amplitude of the controlled TS-wave ( $\tilde{Y}_{i+1}$ ) is smaller than a ( $\tilde{Y}_i$ ), a controller parameter signal takes a positive value and the operating parameter changes adding a step size. Otherwise, if the amplitude ( $\tilde{Y}_{i+1}$ ) increases with time, the step size of the operating parameter will be reduced ( $\Delta\Psi_i = 0.2\Delta\Psi_{i-1}$ ) and the controller parameter takes a negative value.
4. Return to step 2 again until the controlled parameter remains unchanged in time, i.e. the convergence error  $\epsilon \approx 0$ .

The procedure is similarly applied to all operating parameters. Convergence is obtained within only a few iterations.

The amplitude of the waves downstream of the control actuator is analyzed using the signal of the second sensor ( $S_2$ ), positioned at  $x = 550\text{mm}$ . At the beginning of each cycle, an algorithm alters the controlled parameter in an iterative process based on the comparison of the amplitude of the previous cycle and the actual amplitude to determine

Table 1: Optimization parameters using CLC.

Voltage	$\Delta bf$	signal	Phase shift	$\Delta \Phi$	signal
5000.00	500.00	+	180.00	20.00	+
5500.00	500.00	+	200.00	20.00	+
6000.00	500.00	+	220.00	20.00	+
5600.00	100.00	-	204.00	04.00	-
5520.00	020.00	+	208.00	04.00	+
5540.00	020.00	+	212.00	04.00	+
5560.00	020.00	+	216.00	04.00	-
5580.00	020.00	+	220.00	04.00	-
5564.00	004.00	-	216.80	00.80	+
5568.00	004.00	-	217.60	00.80	+
5564.80	000.80	+	218.40	00.80	+
5565.60	000.80	-	218.20	00.80	+
5564.90	000.16	-	218.56	00.16	-

whether the last step improved the cancellation result. If the last step resulted in an improvement the controlled variable is altered again in the same direction. Only one parameter can be controlled at a time. The alteration of the phase shift  $\phi = 180^\circ - 340^\circ$  produces different cancellation results, as illustrated in Fig. 4. At about  $\phi = 210^\circ$  the best attenuation of TS-waves can be observed. In this diagram, the phase shift has been continuously changed in order to demonstrate the influence of this parameter.

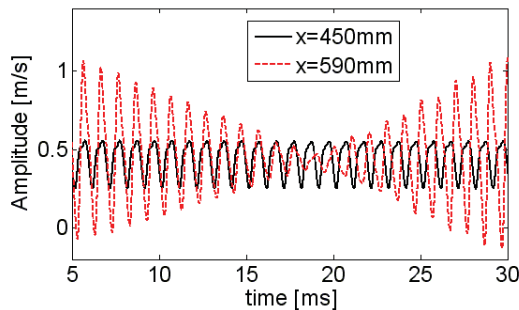


Figure 4: Phase-shift  $\Phi = 180 - 340$  variation.

Table 1 shows the data evaluated during the optimization of voltage and phase-shift processes using the algorithm developed in the current paper. In this case  $\Delta bf_0 = 500V$ ,  $bf_0 = 5000V$ ,  $\Delta\Phi_0 = 180^\circ$  and  $\Phi_0 = 20^\circ$ . The convergency criterion is given by

$$f_{opt} = f(\Phi_{max}, bf_{max}) - f(\Phi_{min}, bf_{min}) \leq 2 \times 10^{-1}, \quad (3)$$

because it is not computationally expensive and yields satisfactory results.

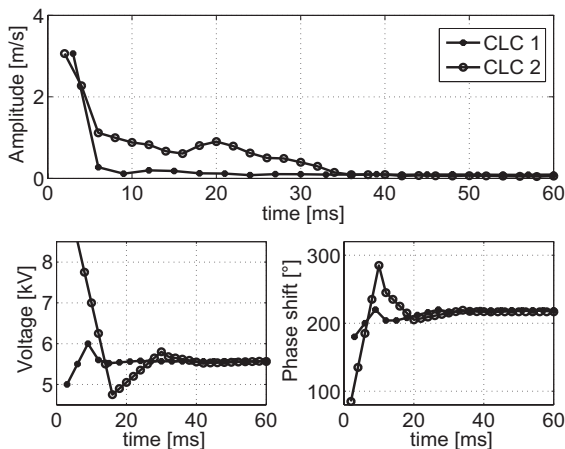


Figure 5: Comparison of amplitude, phase shift and voltage using CLC method.

Neldermead method

Table 2: Optimization parameters using Neldermead method.

k	Best point	Good point	Worst point
1	f(6050.00,210.00)	f(6350.00,220.00)	f(5850.00,230.00)
2	f(5550.00,220.00)	f(5850.00,230.00)	f(6050.00,210.00)
3	f(5550.00,220.00)	f(5850.00,230.00)	f(5350.00,240.00)
4	f(5550.00,220.00)	f(5875.00,217.50)	f(5850.00,230.00)
5	f(5550.00,220.00)	f(5575.00,207.50)	f(5875.00,217.50)
6	f(5550.00,220.00)	f(5575.00,207.50)	f(5250.00,210.00)
7	f(5550.00,220.00)	f(5575.00,207.50)	f(5408.00,211.80)
8	f(5562.50,213.80)	f(5479.00,215.90)	f(5550.00,220.00)
9	f(5562.50,213.80)	f(5479.00,215.90)	f(5491.50,209.60)
10	f(5562.50,213.80)	f(5506.10,212.20)	f(5479.00,215.90)
11	f(5562.50,213.80)	f(5506.10,212.20)	f(5589.60,210.10)
12	f(5562.50,213.80)	f(5506.10,212.20)	f(5506.65,214.45)

The Nelder-Mead (Neldermead) method is a simplex method for finding a local minimum of a function of several variables. It's discovery is attributed to J. A. Nelder and R. Mead (1965). For two variables, a simplex is a triangle, and the method is a pattern search that compares function values at the three vertices of a triangle. The worst vertex, where  $f(x, y)$  is largest, is rejected and replaced with a new vertex. A new triangle is formed and the search is continued. The process generates a sequence of triangles (which might have different shapes), for which the function values at the vertices get smaller and smaller. The size of the triangles is reduced and the coordinates of the minimum point are found.

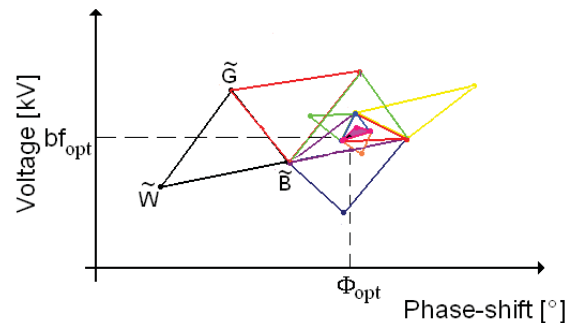


Figure 6: The sequence of triangle converging to the optimum point for the Nelder-Mead method.

Applying the Nelder-Mead method to optimize the operating parameters of the plasma actuator using sinusoidal modulation, three vertexes are first simulated using the FASTEST-3D code. The amplitude of the TS-waves (function) are then evaluated at these vertexes. The data are presented in table 2. The initial vertex  $\hat{B} = (6050V, 210^\circ)$  corresponds to the parameters where the amplitude of the TS-waves are more efficiently reduced in the first iterations. The worst vertex  $\hat{W} = (5850V, 230^\circ)$  attenuates the function badly compared with another two vertices and so will be rejected and replaced with a new vertex. The process generates a sequence of triangles, for which the function correspondent of the parameters at the vertices get smaller and smaller. The process stops when the objective function is reached, in other words, the amplitude of TS-waves are completely reduced. The diagram of the Fig. 6 gives more details about the steps of the triangle process generated in the algorithm during the optimization process.

The influence of the initial points affects the temporal evaluation, but the optimum points do not change with them. Fig. 7 shows two different initial points using Nelder-Mead method. The evaluation points are chosen distinctly apart and at the same time the convergency criterium was satisfied for both cases. This shows that the optimum points are found independently of the chosen initial point.

NEUVOA method

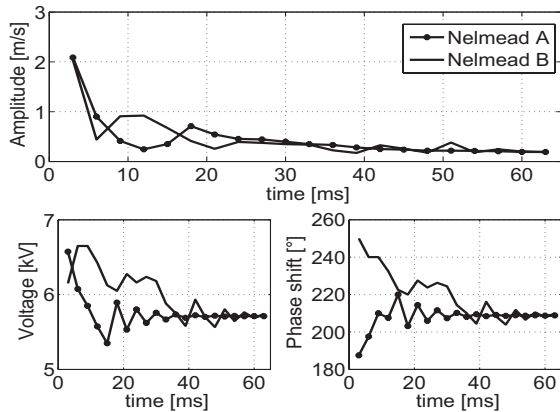


Figure 7: Comparison of amplitude, phase shift and voltage for two different initial points using Nelder-mead method.

NEWUOA seeks the minimal value of a function  $F(x)$ ,  $x \in R^n$ , when  $F(x)$  can be calculated for any vector of variables  $x$ . In each iteration a quadratic model  $Q$  is created using  $m$  interpolation points of  $F$ .

As input NEWUOA expects an initial vector  $x_0 \in R^n$ , in our case it is  $n = 2$  and  $x_0 = (\text{voltage, phaseshift})$ . The number of interpolation conditions is selected as  $m = 2n + 1 = 5$ , because NEWUOA shows for this value a good optimization behaviour. The interpolation points are chosen inside a neighbourhood (trust-region) of  $x_0$  with range  $\rho_{beg}$ .

With these points an initial quadratic model  $Q$  is created to optimize  $F$ . Then the following iterations are made: The minimum of  $Q$  is computed inside a trust-region. The objective value of this new located point is calculated and is used to update  $Q$  by replacing the actual worst point. Because of this each iteration changes only one of the interpolation points, keeping  $m$  fixed. The  $m$  chosen points are the best vectors of variables at the beginning of the  $k$ -th iteration, which means that their objective function values are the minimal calculated values of  $F$  so far. If the values of the objective function  $F$  stops decreasing, the trust-region radius is reduced. NEWUOA stops if the radius is lower than a given end value. The defined objective function is given by

$$\sum_{j=i}^{i+m-1} \frac{(A(t_{j+1}) - A(t_j))^2}{t_{j+1} - t_j}, \quad (4)$$

where  $A$  is the TS-wave amplitude and  $\lambda = |[t_i, t_{i+m}]|$  with time  $t_i$ . Details can be found in (Powell, 2008).

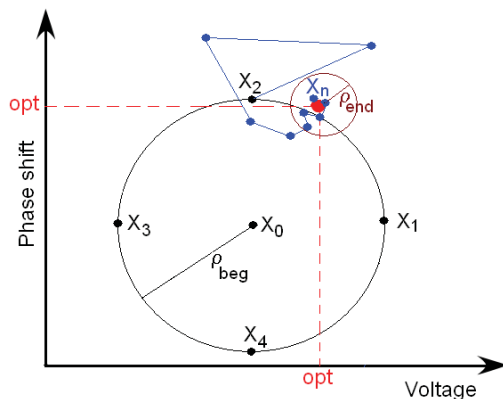


Figure 8: NEWUOA scheme.

Table 3 presents the data of the evaluation points of the

Table 3: Parameter optimizations using NEWUOA method.

$k \times 10^3$	point 1		
	$f(bf, \phi)$	amplitude	$F_{target}$
2	f(6000.00,210.00)	0.428	089.776
4	f(6500.00,210.00)	0.551	251.304
6	f(6000.00,220.00)	0.444	105.150
8	f(5500.00,210.00)	0.256	041.368
10	f(6000.00,210.00)	0.328	092.146
12	f(5536.03,200.00)	0.219	040.132
14	f(5516.10,206.34)	0.172	036.464
16	f(5471.57,205.42)	0.167	034.091
18	f(5474.57,204.96)	0.177	033.349
20	f(5458.42,203.97)	0.160	032.866
22	f(5422.94,205.93)	0.163	030.829

NEWUOA method. The corresponding points of this table are shown in Fig. 8.

Initially the five points are evaluated and the amplitude and the objective function for all points are found. Using these points the initial quadratic model  $Q$  is developed.

The next point is chosen in the trust-region of the optimal point (5500, 210) and is found in (5536.03, 200.00). The point, that has the maximum value of the objective function is discarded, in this example it is (6500, 210), and replaced by (5536.03, 200.00). This one is the new optimal point and the next point is searched in its trust-region and so on.

Minimizing the objective function, the TS-waves are totally attenuated. In this case the best body-force  $bf_{opt} = 5422.94V$  and phase-shift  $\Phi_{opt} = 205.93^\circ$  was found, corresponding to the minimal objective function value  $F_{target} = 30.829$ .

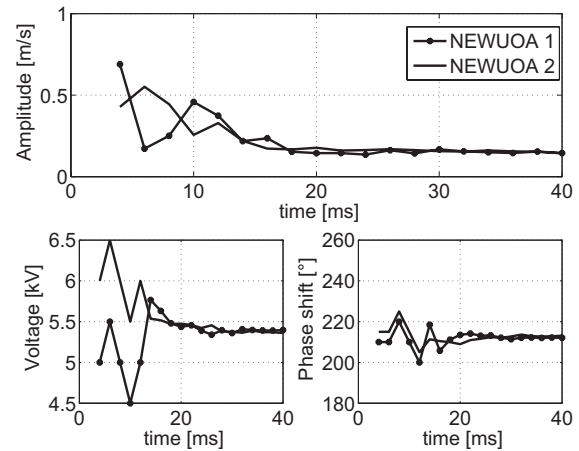


Figure 9: Comparison of amplitude, phase shift and voltage for two different initial points using NEWUOA method.

Fig. 9 shows two independent simulations using different initial points to start the NEWUOA method. For the first simulation:  $x_1 = (5000, 210)$ ;  $x_2 = (5500, 210)$ ;  $x_3 = (5000, 220)$ ;  $x_4 = (4500, 210)$  and  $x_5 = (5000, 200)$  and for second simulation, the initial parameters are given in table 3. Observe that in both cases the optimum parameters are found in approx. 20ms. The best parameter in the second case is  $x_{opt} = (5389.16, 212.26)$ . The temporal evolution of the velocity profile in the second sensor is described in Fig. 10. In this case a reduction of 96% of the TS-wave-amplitude is found, as confirmed in the upper diagram of Fig. 9.

A comparison between all methods in the forward sections at 90mm downstream the control actuator points is shown in Fig. 11. The optimization methods presents reasonable velocity of convergency and the results show very

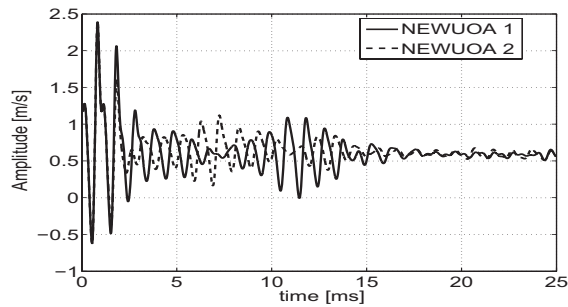


Figure 10: Comparison with two initial points using NEWUOA at  $x=590\text{mm}$ .

good agreement, reducing the TS-wave amplitude by 95% in all three cases.

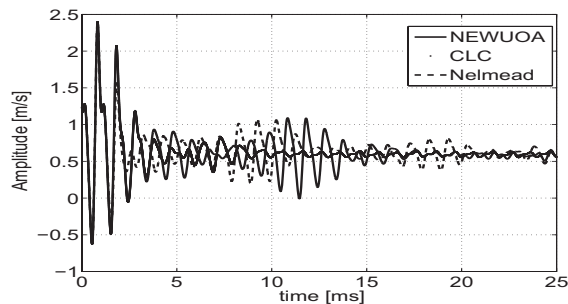


Figure 11: Amplitude of TS-wave comparison for three optimization methods.

## VELOCITY SPECTRA

The velocity spectra for the flow with the actuators on are shown in Fig. 12. They reveal two important features. The first is the large spectral peaks at the unsteady excitation frequency of the TS-waves and higher harmonics. The second important feature is the similarity in the magnitude of background noise in both cases. The spectra give more detailed information about the frequency content and the shape of the fluctuations with and without control actuator using the optimal parameters. At the first position at  $x=450\text{mm}$  (upstream of the control actuator) the harmonics have the same amplitude in both cases and the peaks show the disturbances generated by the excitor. At  $x=590\text{mm}$ , the harmonics have a high amplitude without control actuator because the flow already is in a transitional process. However, at the same stream-wise position, the harmonics are reduced significantly and the fifth peak is not present at all when the control actuator is turned on. If the active wave cancellation is operating, the velocity-spectra of the second sensor signal shows remarkably reduced amplitudes compared to the case without active wave cancellation (AWC). A mean cancellation of about 16dB can be observed in the fundamental TS frequency range (110Hz), which corresponds to a reduction of the TS-amplitudes at least of 88%.

## CONCLUSIONS

Plasma actuators reduce the amplitude of TS-waves significantly in a flat-plate boundary layer using sinusoidal modulation leading to a delayed transition. The AWC closed-loop circuit is operated autonomously in the numerical simulations. It is found that only two operating parameters must be controlled in order to reduce the amplitude

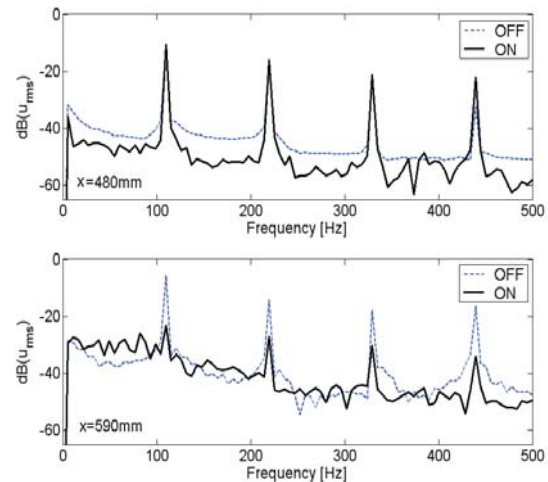


Figure 12: Velocity spectra at two streamwise locations with and without control actuator. The data was extracted from  $y = 0.5 \delta_{99}$ .

of TS-waves. The best phase shift and body force found for 8m/s velocity was around  $\Phi = 210^\circ$  and  $bf = 5.5kV$ , respectively.

Optimizing only two parameters of plasma actuator the method developed in this work yielded better convergence compared with NELMEAD and NEWUOA methods. However, increasing the number of parameters to be considered in the optimization the CLC method becomes invariable computationally and the other two algorithms maintain the same velocity of convergence. The NEWUOA method is more precise than the other two optimization methods since this method has an approximation of second order.

## REFERENCES

- Saric, W.S., 2007, "Boundary-Layer Stability and Transition". In *Springer Handbook of Experimental Fluid Mechanics*. Eds. C. Tropea, A.L. Yarin, J. Foss, Springer-Verlag, Heidelberg.
- Nelder, J. A. and Mead, R., 1965, "A Simplex Method for Function Minimization". *The Computer Journal*, **7**: 308-313.
- Powell, M. J. D., 2008, "Developments of NEWUOA for minimization without derivatives", *IMA Journal of Numerical Analysis*, **28**: 649 - 664.
- Grundmann, S., Klumpp, S. and Tropea, C., 2006, "Experimental and Numerical Investigations of Boundary-Layer Influence using Plasma-Actuators". *Notes on Numerical Fluid Mechanics and Multidisciplinary Design*, **95**.
- Jayaraman, B. and Shyy, W., 2003, "Flow Control And Thermal Management Using Dielectric Glow Discharge Concepts", *AIAA 2003-3712*.
- Grundmann, S., Klumpp, S., Tropea, C., 2006, "Stabilizing a laminar boundary-layer using plasma-actuators", *25th International Congress of the Aeronautical Sciences*, Hamburg, September 3 - 8, ID255.
- Grundmann, S., 2008, "Transition Control using Dielectric Barrier Discharge Actuators", Ph.D Thesis, TU-Darmstadt.
- Quadros, R., Grundmann, S., Tropea, C., Albrecht, T. and Grundmann, R., 2009, "Numerical investigations of the boundary-layer stabilization using DBD plasma actuators", *Flow, Turbulence and Combustion - Special Issue ETMM7*.